Am J Cancer Res 2023;13(8):3832-3852
www.ajcr.us /ISSN:2156-6976/ajcr0150187

Original Article

Inhibition of protein kinase C isozymes causes immune profile alteration and possibly decreased tumorigenesis in bladder cancer

Deepika Trehan[1,2], Ranbala Kumari[1,3], Jyoti Sharma[1], Sri Harsha Satuluri[1], Satya Sahay[1], Nitu Kumari Jha[1], Janendra K Batra[2], Usha Agrawal[1]

[1]ICMR-National Institute of Pathology, New Delhi, India; [2]Jamia Hamdard University, New Delhi, India; [3]Amity University, Noida, UP, India

Received March 17, 2023; Accepted June 23, 2023; Epub August 15, 2023; Published August 30, 2023

Abstract: Protein kinase C (PRKC) isozymes activate many signaling pathways and promote tumorigenesis, which can be confirmed by masking the kinase activity. In the present study, the kinase activity of PRKC ε and ζ isozymes was masked by siRNA in bladder cancer, and the consequent gene profile was evaluated. Here, we show that the commonly dysregulated genes affected by both the isozymes were the chemokines (CXCL8 & CXCL10), adhesion molecules (ICAM1, SPP1, MMP3, VEGFA) and mutated isoform of TP53. As these same genes were upregulated in bladder cancer patients, the activity of the kinase in downregulating them is confirmed. These genes are associated with regulating the tumor microenvironment, proliferation and differentiation of cancer cells and poor prognosis. The effect of kinase masking in downregulating these genes in bladder cancer indicates the benefits PRKC inhibitors may have in managing these patients.

Keywords: Protein kinase C, bladder cancer, chemokines, adhesion molecules, TP53, siRNA knockdown

Introduction

Protein kinase C (PRKC) isozymes are known signal transducers that play an important role in normal physiology and numerous diseases, including cardiovascular, neurological, and proliferative dysfunctions. Their significance in oncogenesis is well documented through the regulation of several signalling pathways involved in differentiation, survival, and apoptosis [1]. This family of serine-threonine kinases comprises of three groups of isozymes with unique biochemical properties: classical/conventional or calcium-dependent cPRKCs (α, βI, BII, γ); novel or calcium-independent nPRKCs (δ, ε, η, θ) and atypical PRKCs (ζ & Cı) [2]. Phosphorylation as a result of PRKC action can lead to conformational changes in the target which may modulate biochemical functions and fine-tune tightly regulated biological network [3, 4]. Deregulated kinase signaling has been implicated in the hallmarks of cancers such as differentiation, progression and apoptosis [5]. Although PRKCs exhibit strong functional selectivity in cells due to their distinct intracellular location and differential access to substrates, they exhibit high homology and similar substrate specificity in vitro [6]. Elevated PRKC activity was found to be associated with the increased metastatic or invasive potential of mouse melanoma cells [7], hepatocellular carcinoma [8], human gastric cancer cells [9] and human urinary bladder carcinoma cells [10]. This is well illustrated by members of the novel PRKC family and atypical PRKC family, namely PRKC-ε and PRKC-ζ, which share the similarity in their catalytic domain and exert similar effects, particularly in the context of metastasis and survival [2, 6, 11-13]. Specific PRKC inhibitors have thus been shown to suppress the invasive and/or metastatic potential of cancer cells by reducing cell motility [10, 11], chemotaxis [14] and expression of proteolytic enzymes [15]. Many PRKC inhibitors, such as Imatinib, the first-generation inhibitor, Bcr-Abl, the second-generation, including dasatinib, bosutinib and nilotinib, have been approved for cancer treatment. Other tyrosine kinase inhibitors (TKI's), such as osimertinib, are being taken up as irreversible inhibitors against various

Table 1. Bladder cancer cell lines used in the study

Cell Line	Disease (Urinary bladder cancer)
5637	Grade II, carcinoma
J82	Grade III, carcinoma
TCCSUP	Grade IV, transitional cell carcinoma
T24	Transitional cell carcinoma

tumors [16]. Due to the varied role played by PRKCs, studying the effect of PRKC inhibition on signaling pathways may give a deeper understanding of cancer biology. Therefore, we conducted PRKC-ε and PRKC-ζ si-RNA inhibition followed by genome wide analysis using Bladder carcinoma (BC) cell lines as a model. The identification of the underlying mechanism of PRKC inhibition of bladder cancer cells could help to discover targets for designing inhibitors to treat urothelial bladder carcinoma.

This study was designed to conduct si-RNA knockdown of PRKC-ε & ζ isozymes followed by cDNA microarray analysis to identify the common differentially expressed genes (DEGs) after the knockdown. Validation of hub genes has been achieved by analyzing mRNA expression of different grade bladder cancer cells and the expression of bladder tumor tissues from TCGA. This study provides an insight into the regulation of novel genes by PRKC isozymes in bladder cancer.

Methodology

Cell culture and transfection with siRNAs

Cell transfection for PRKC-ε & ζ was performed in 6-well tissue-culture flasks. The cells (**Table 1**) were allowed to grow in a medium containing 5% FBS without antibiotics upto 50-75% confluency. Before transfection, the medium was aspired and 400 µL of transfection medium (opti-MEM) containing 10 mMol siRNA and 30 µL of Lipofectamine 2000 (1:1 ratio) were added followed by incubation at 37°C in a CO_2 incubator upto 48 hrs. Transfection efficiency was checked through qRT-PCR and Western blot analysis. All experiments were performed in triplicate.

Quantitative real time - PCR

The cells were harvested for RNA extraction before and after transfection. Total RNA was extracted from all the cell lines using the RNeasy Micro Kit (cat. No.: 74004, Qiagen). cDNA was synthesized at 42°C for 40 min and 85°C for 5 min, and was used as a template for the amplification with pre-denaturation at 94°C for 2 min, 30 cycles of denaturation at 94°C for 30 sec, annealing at 60°C for 30 sec and extension at 72°C for 30 sec, then final extension at 72°C for 2 min (Applied Biosystems™, cat No: 4368814). qRT-PCR was performed using TaqMan polymerase (Applied Biosystems™, cat No.: 4364340) All experiments were performed in quadruplicates.

Western blot analysis

The cells were treated with RIPA buffer on ice for 15 mins, followed by 45 sec pulse sonication and 12000 RPM centrifugation for protein extraction. The supernatant was collected and utilized for Western blot development pre and post transfection. The protein was segregated through vertical SDS-PAGE followed by transfer to the nitrocellulose blot. The blot was probed with PRKC-ε & ζ antibodies for the identification of expression in each sample and β-actin as loading control.

Protein kinase C-ε & ζ activity assessment in cell lines

The concentration of protein was defined through traditional BCA method. The Enzyme-linked Immunosorbent Assay Kit (MBS2701804 and MBS2019639, My-BioSource's) was utilized to assess pre and post silenced kinase activity of PRKC-ε & ζ isozymes of each cell lines in triplicates. The ELISA was conducted as per manufactures protocol and the reading was obtained at 450 nm.

Microarray experiment

RNA quality was checked through a Bioanalyzer (Agilent RNA 6000 Pico Kit, cat No.: 5067-1513). The RNA samples which passed the quality (RIN ≥ 7) were processed for cDNA microarray analysis. A total of 12 samples including the cancer cell lines and the knockdown set of ($PRKC\varepsilon^-$ and PRKCζ) were processed in duplicate using the Sure Print G3 Human Gene Expression v3 Microarray Kit, 8 × 60K. Data was obtained as text (.txt) files.

Identification of differentially expressed genes

Normalization of curated data was conducted in Genespring version 14.9.1. on the isonomic variables and GraphPad Prism version 8 was

used to compare means and calculate paired/unpaired Student's t-test. For each probe set, the $\log_2$ (treatment/control) ratio was computed, and *p* values from a one-way analysis of variance were then corrected for false discovery rate (FDR) using the Benjamin-Hochberg method. Probe sets were filtered for single-gene analysis if expression varied by 2-fold in any of the conditions studied and if the *p*-value for the analysis of variance was 0.05. To find differentially expressed genes, the expression profiles of samples with PRKC expression ($PRKC^+$) compared to samples with PRKC knockdown ($PRKC^-$) were curated. The upregulated and downregulated sets were separated using data from all statistically significant probe sets in an ANOVA one-way Benjamin-Hochberg analysis.

Functional enrichment analysis

The common gene set of upregulated and downregulated genes were processed for GO, KEGG and Hallmark gene sets. For each PRKC isozyme, samples from two classes were compared: PRKC expressing versus PRKC-depleted ($PRKC^+$ vs $PRKC^-$). To identify probable mechanisms and important biological processes connected to overlapping DEGs, functional enrichment analysis and pathway enrichment analysis of genes were carried out with the ClueGO version 2.5.6.

Construction of PPIs

A PPI of the common gene set of upregulated and downregulated genes was generated with STRING, version 11 [50] and visualized using Cytoscape (version 8.0; http://cytoscape.org/) [51]. The Cytoscape plugin "MCODE" generated cluster modules and clusters with score > 5 and number of nodes ≥ 10 was considered significant. Hub genes were identified based on centrality values such as closeness, degree, EPC, MCC, and MNC. The hub genes were ranked according to the selected centrality values and the most interacting genes were identified. To discover the important biological processes connected to it, the significant modules were further processed for gene ontology (GO). GO categories and overrepresented pathways were identified using ClueGO version 2.5.6 [52]. Signalling pathways were systematically examined using the Kyoto Encyclopedia of Genes and Genomes (KEGG, http://www.genome.jp/) enrichment database [53]. In choosing GO terms and pathways, the advanced statistical criteria were min#genes = 3, %gene/term = 4. Additionally, a two-sided hypergeometric test was used to do the enrichment/depletion and *p* value adjustment methods. Kappa score for GO term/pathway network connection was set to 0.4. The cut-off value for significance (*p*-value) was set to 0.05, with the GO tree interval level set at 3 to 8.

Validation of the hub genes

The mRNA expression levels of the screened hub genes were validated through qRT-PCR in bladder cancer cell lines and TCGA Bladder cancer datasets (BLCA) consisting of 409 BLCA cases and 19 normal bladder samples. The expression of these genes was analysed with the Tukey HSD (honest significant difference) test. A co-relation analysis was conducted by comparing the TCGA reported PRKC-ε & ζ expression and the hub genes. The protein expression of hub genes in bladder tumor tissue and normal tissues was determined using the Human Protein Atlas (HPA) [54], and the commercially available TMA (NBP3-11846 - Human Bladder Tissue MicroArray Cancer).

Survival analysis of hub genes

The survival analysis of hub genes in BLCA was analysed using TCGA database [55]. A Cox proportional hazards model $P < 0.05$ was considered significant, and associated data analysis was displayed in a survival plot.

Statistical analysis

The identification of DEG's were done using moderate t-test, with a cut-of criteria logFC > 1 or logFC > -1 and *p*-value < 0.05. The construction of PPI network was obtain using maximum number of interactors = none/query proteins only and confdence score ≥ 0.4. The GO biological attributes were annotated with min#genes = 3 and %gene = 4 in GO term/pathway selection. The GO tree interval level was set as 3, max level as 8 and *p*-value ≤0.05 as the cut-of criterion of significance. The mean ± SD of the hub genes was assessed using Tukey's Honest Significant Difference (HSD) test and *p* values of the pairwise comparisons are indicated as significant (***P). The correlation analysis was calculated using Spearman correlation

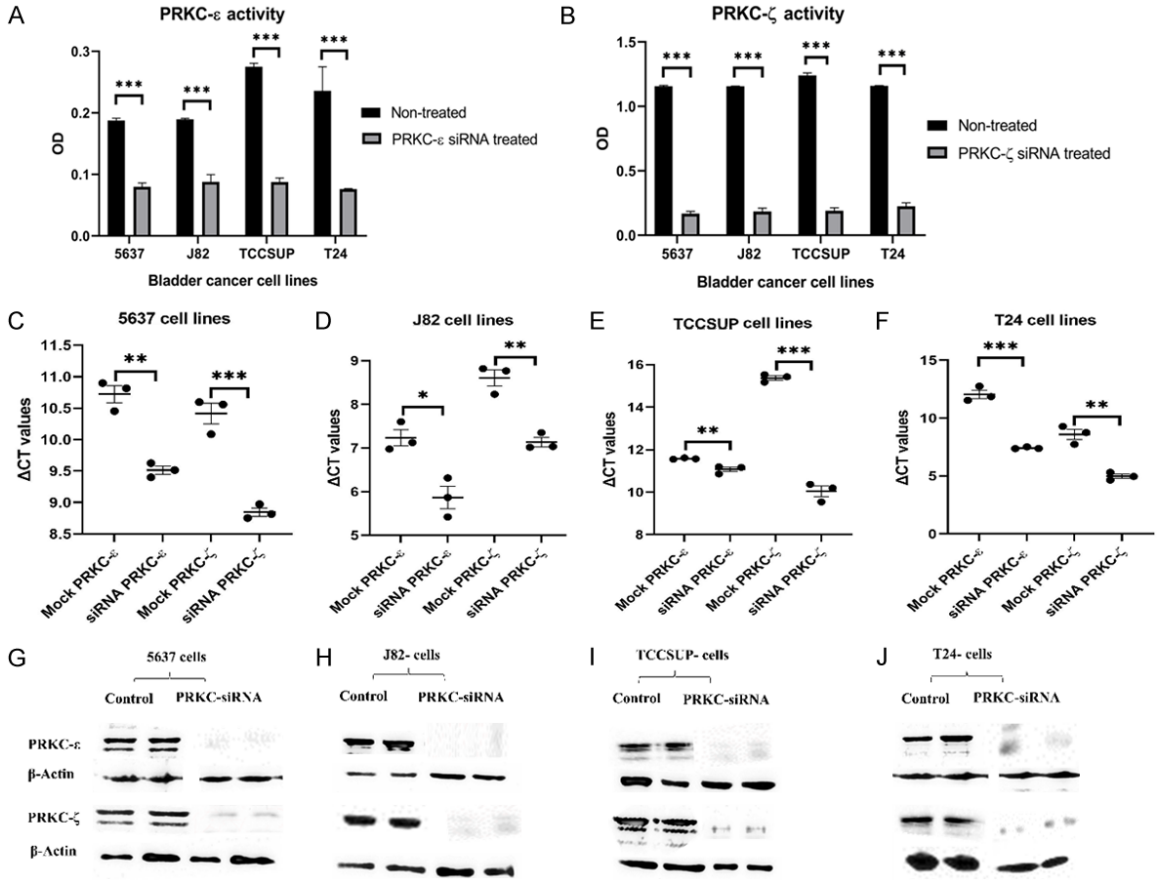

Figure 1. Expression of kinase isozymes based on activity and post silencing events in bladder cancer cell lines. (A) PRKC-ε concentration in pre and post silenced cell lines with a range of 17 to 4 ng/ml. (B) PRKC-ζ concentration in pre and post silenced cell lines with a range of 19 to 0.9 ng/ml. mRNA expression of PRKC ε & ζ in pre and post inhibition among bladder cancer cell line. (C) 5637 (Mock & siRNA PRKC-ε & PRKC-ζ), (D) J82 (Mock & siRNA PRKC-ε & PRKC-ζ), (E) TCCSUP (Mock & siRNA PRKC-ε & PRKC-ζ), (F) T24 (Mock & siRNA PRKC-ε & PRKC-ζ) were found to be significantly downregulated (*p* value: * < 0.05, ** < 0.01, *** < 0.001). Absence of protein bands in comparison to control due to siRNA knockdown was observed in (G) 5637, (H) J82, (I) TCCSUP and (J) T24 (β-actin was used as a loading control).

to examine potential associations between the expression levels of differentially expressed genes and the kinase activity. The survival analysis was assessed through Cox proportional hazards model with significance at P < 0.005.

Results

Kinase Isozymes activity

The activity of each isozyme was observed in terms of concentration (ng/ml) and it was found that the non-invasive cell lines 5637 and J82 had an OD of 0.13 and 0.18 in pre silenced PRKC-ε samples with a significant downregulation to 0.08 post silencing (**Figure 1A**). Similarly, the invasive cell lines, TCCSUP and T24 had a higher OD of 0.27 and 0.24 in pre-silenced cells, which dropped significantly to 0.09 and 0.08 respectively (**Figure 1A**). Upon observing the PRKC-ζ concentration in pre silenced cells, it was found to be, almost equivalent in all the cell lines (5637 = 1.15, J82 = 1.15, TCCSUP = 1.24 and T24 = 1.16), which dropped to non-detectable range post silencing among all the cell lines (**Figure 1B**).

PRKC ε and ζ knockdown

The gene expression of PRKC-ε and PRKC-ζ in bladder carcinoma cell lines 5637 (Grade II carcinoma), J82 (Grade III carcinoma) TCCSUP (Grade IV TCC) & T24 (TCC) was evaluated, before and after transfection with si-RNA by qRT-PCR and western blot analysis. A significant gene downregulation post PRKC-ε and ζ

silencing was observed at mRNA (**Figure 1C-F**) and protein levels (**Figure 1G-J**) in all bladder cancer cells.

Differentially regulated genes (DEG's) in PRKC-ε & ζ knockdown

Using a cut-off of FDR > 2 and P < 0.05, a total of 1959 and 11537 genes were found to be upregulated and downregulated (**Figure 2A**) respectively in cells with siRNA mediated PRKC-ε knockdown. Similarly, among siRNA mediated PRKC-ζ knockdown a total of 892 and 1332 genes were found to be upregulated and downregulated respectively (**Figure 2B**). While 1824 and 757 genes were distinguished under unique upregulated genes (**Figure 2C**), 11091 and 886 genes (**Figure 2D**) were identified as unique downregulated for PRKC-ε and ζ knockdown respectively. A total of 134 upregulated genes and 445 down-regulated genes were found to be commonly dysregulated with knockdown of both isozymes bringing the total common dysregulated genes to 579. These sets were marked under group A (PRKC ε & ζ common upregulated genes) and group B (PRKC ε & ζ common downregulated genes).

Protein-protein interaction (PPI) network analysis

The 579 common dysregulated genes generated a PPI network of 353 nodes of enrichment *p*-value: < 1.0e-16 in Cytoscape (**Figure 2E**). The remaining nodes were in small clusters or single, not interacting with any other genes. The big network of 353 nodes was analyzed for modules with a score of > 5 and the number of nodes ≥ 10 in MCODE. A total of 3 modules were constructed, out of which only one module with MCODE score of 16.316 (20 nodes, 155 edges) was identified to be statistically significant (**Figure 2F**).

HUB gene identification

Out of 19, a set of 15 hub genes were identified as the most interacting genes based on centrality values (**Table 2**; **Figure 2G**). The genes included CSF3, LCN2, VEGFA, SPP1, CXCL8, CD86, CXCL2, TP53, CXCL10, MMP1, CX3CL1, MMP3, IL6, CCL3 and ICAM1.

HUB gene basal expression through qRT-PCR

To verify the identified hub genes dependability of PRKC, qRT-PCR was conducted on control and knockdown samples of four different bladder cancer cell lines. A total of 12 genes, including CSF3, VEGFA, SPP1, CXCL2, TP53, CXCL10, CX3CL1, MMP3, IL6, CCL3, ICAM-1 and CXCL8 showed statistically significant downregulation in all the four grades of bladder tumor. Total 3 genes, LCN2, CD86, and MMP1 were found to be upregulated in all the tested cell lines. The differences in expression levels of each hub gene between control and knockdown samples are shown as bar plots in **Figure 3A**.

mRNA expression analysis of hub genes from TCGA

The mRNA expression of the identified hub genes was explored using TCGA database in tumor and normal cases, and the levels of LCN2, VEGFA, SPP1, CD86, TP53, CXCL10, CXCL8, MMP1, CCL3, MMP3, ICAM1 were found to be significantly upregulated in TCGA BLCA database. CSF3, CXCL2, IL6 and CX3CL1 showed significant downregulation (**Figure 3B**) in comparison to the normal bladder cases.

Co-relation analysis of hub genes with PRKC-ε & ζ expression

The expression of PRKC-ε was co-related with the expression of hub genes in TCGA data. The results of the Spearman correlation test indicated that an increased expression of PRKC-ε is statistically significant and in a negative correlation with the expression of CSF3, LCN2, SPP1, CXCL8, CD86, CXCL2, CXCL10, MMP1, MMP3, CCL3 and ICAM1 genes (**Figure 3C**). Similarly, PRKC-ζ expression shows the statistical significance and inverse correlation with CSF3, SPP1, CX3CL1, CXCL8, VEGFA, CD86, CXCL2, CXCL10, TP53, MMP1, MMP3, IL6, CCL3, LCN2 and ICAM1 (**Figure 3D**). The genes which are inversely regulated by both the isozymes are CSF3, SPP1, CXCL8, CD86, CXCL2, CXCL10, MMP1, MMP3, CCL3 and ICAM1.

Regulatory functions identification

The 15 hub genes show significant enrichment under biological regulatory functions (GO category) for positive regulation of leukocyte migration (CCL3, CX3CL1, CXCL10, CXCL8, ICAM1, IL6, VEGFA), cellular response to liposaccharide (CCL3, CD86, CSF3, CX3CL1, CXCL10, CXCL2, CXCL8, ICAM1, LCN2), regulation of neuroblast formation (CX3CL1, TP53, VEGFA) (**Figure 3E**). Upon KEGG pathway analysis IL-17 signalling (CSF3, CXCL1, CXCL10, CXCL2, CXCL8, IL6,

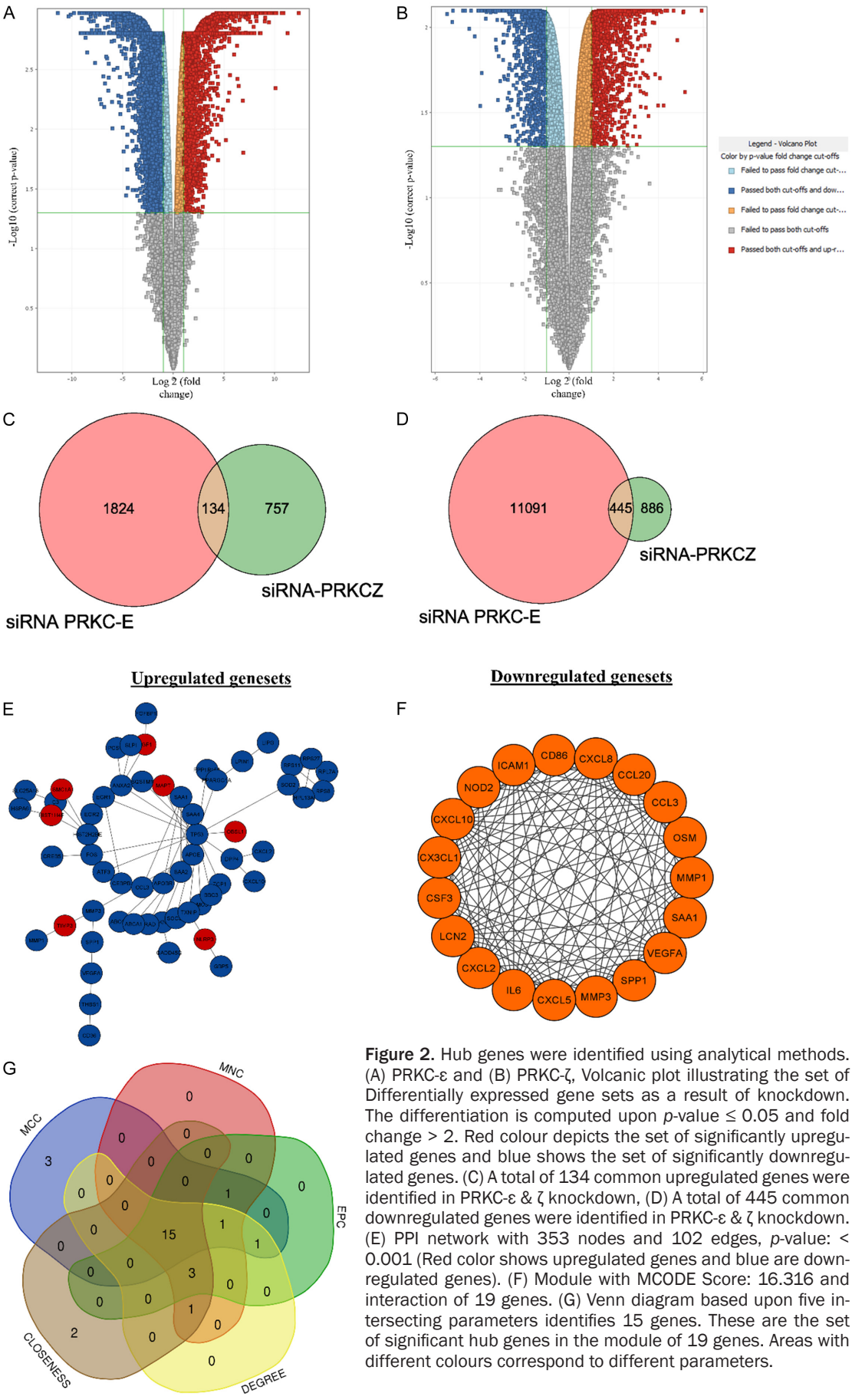

Figure 2. Hub genes were identified using analytical methods. (A) PRKC-ε and (B) PRKC-ζ, Volcanic plot illustrating the set of Differentially expressed gene sets as a result of knockdown. The differentiation is computed upon *p*-value ≤ 0.05 and fold change > 2. Red colour depicts the set of significantly upregulated genes and blue shows the set of significantly downregulated genes. (C) A total of 134 common upregulated genes were identified in PRKC-ε & ζ knockdown, (D) A total of 445 common downregulated genes were identified in PRKC-ε & ζ knockdown. (E) PPI network with 353 nodes and 102 edges, *p*-value: < 0.001 (Red color shows upregulated genes and blue are downregulated genes). (F) Module with MCODE Score: 16.316 and interaction of 19 genes. (G) Venn diagram based upon five intersecting parameters identifies 15 genes. These are the set of significant hub genes in the module of 19 genes. Areas with different colours correspond to different parameters.

Table 2. Top 20 genes of modules evaluated using 5 calculation methods (MCC, MNC, Degree, EPC, and Closeness)

Gene	*MCC*	*Gene*	*MNC*	*Gene*	*EPC*	*Gene*	*DEGREE*	*Gene*	*CLOSENESS*
IL6	1.13E+09	IL6	72	IL6	40.97	IL6	72	IL6	139.95
CXCL8	1.13E+09	TP53	51	CXCL8	39.34	TP53	56	TP53	129.93
CXCL1	1.13E+09	CXCL8	47	VEGFA	38.78	CXCL8	47	VEGFA	122.60
VEGFA	1.13E+09	VEGFA	46	TP53	37.37	VEGFA	46	CXCL8	122.30
CCL3	1.13E+09	ICAM1	38	ICAM1	37.30	ICAM1	38	ICAM1	118.21
CXCL10	1.13E+09	APOE	35	CXCL1	36.02	APOE	35	APOE	116.69
ICAM1	1.13E+09	CXCL10	33	CCL3	35.61	CXCL10	33	CXCL10	111.98
CXCL5	1.08E+09	CXCL1	32	CXCL10	35.55	CXCL1	32	CXCL1	111.53
MMP3	1.05E+09	CCL3	29	CXCL2	35.25	CD86	30	SPP1	109.33
LCN2	1.05E+09	CXCL2	29	MMP3	34.21	CCL3	29	MMP3	108.33
CXCL2	1.04E+09	CD86	29	CSF3	34.04	CXCL2	29	CCL3	107.51
CCL20	1.04E+09	CSF3	28	APOE	33.14	CSF3	28	CSF3	107.46
CSF3	6.00E+08	CCL20	27	LCN2	32.73	FOS	28	FOS	107.15
MMP1	5.28E+08	LCN2	26	CCL20	32.37	CCL20	27	CEBPB	106.84
SPP1	8.22E+07	MMP3	25	SPP1	31.79	SPP1	27	CD86	106.13
CX3CL1	8.02E+07	FOS	25	MMP1	31.26	MMP3	26	CXCL2	105.93
CD86	4.22E+07	CEBPB	25	CD86	30.22	LCN2	26	LCN2	105.85
SAA1	7308145	SPP1	24	CEBPB	29.99	CEBPB	25	MMP1	105.15
OSM	4072519	MMP1	21	FOS	29.96	MMP1	22	PPARGC1A	104.20
TP53	1573575	EGR1	19	CXCL5	29.32	EGR1	20	EGR1	103.10
NOD2	1451652	CXCL5	18	OSM	28.48	OSM	19	THBS1	103.05

LCN2, MMP1, MMP3), TNF signalling pathway (CXCL1, CXCL10, CXCL2, IL6, MMP3), bladder cancer (CXCL8, TP53, VEGFA, MMP1), and Toll like receptor signalling (CCL3, CD86, CXCL10, CXCL8, IL6, SSPI) pathways were enriched (**Figure 3F**).

Prognostic value of hub genes for overall survival

Finally, we investigated the possible predictive value of hub genes by comparing mRNA expression and survival analysis from TCGA using several independent datasets with varying probe IDs for bladder cancer patients. In all, LCN2, VEGFA, TP53, CXCL10, CX3CL1 and MMP3 exhibited better prognosis with < 1 hazard ratio (HR) (**Figure 3G**; **Table 3**). Simultaneously, a significant Cox *p* value was also observed in TP53, CXCL10, ICMA1 and CCL3 (**Table 3**). Genes among upregulated expression in bladder cancer from TCGA database with significant survival rate and HR ratio < 1 are TP53 and CXCL10.

Protein expression of hub genes

In order to validate the hub genes at the protein expression levels, immunohistochemical data of patients were analysed with Bladder tumor tissue data and Normal bladder tissue obtained from the Human Protein Atlas (HPA). The protein expressions of SPP1, VEGFA, TP53, MMP3 and ICAM1 shows > 75% quantity and strong intensity in urothelial bladder cancer and has moderate to no intensity in Bladder normal tissue respectively. CXCL8 shows weak intensity in both urothelial carcinoma and in urothelial cells. The protein expression of CXCL10 in the urothelial bladder cancer is not available through Human Protein Atlas, therefore the expression in tumor was identified through commercially available TMA and the expression was identified to be 75-25% in Bladder tumor tissue and < 25% in Bladder normal tissue (**Figure 3H**).

The evaluation of the TCGA database expression and experimental data (siRNA knockdown)

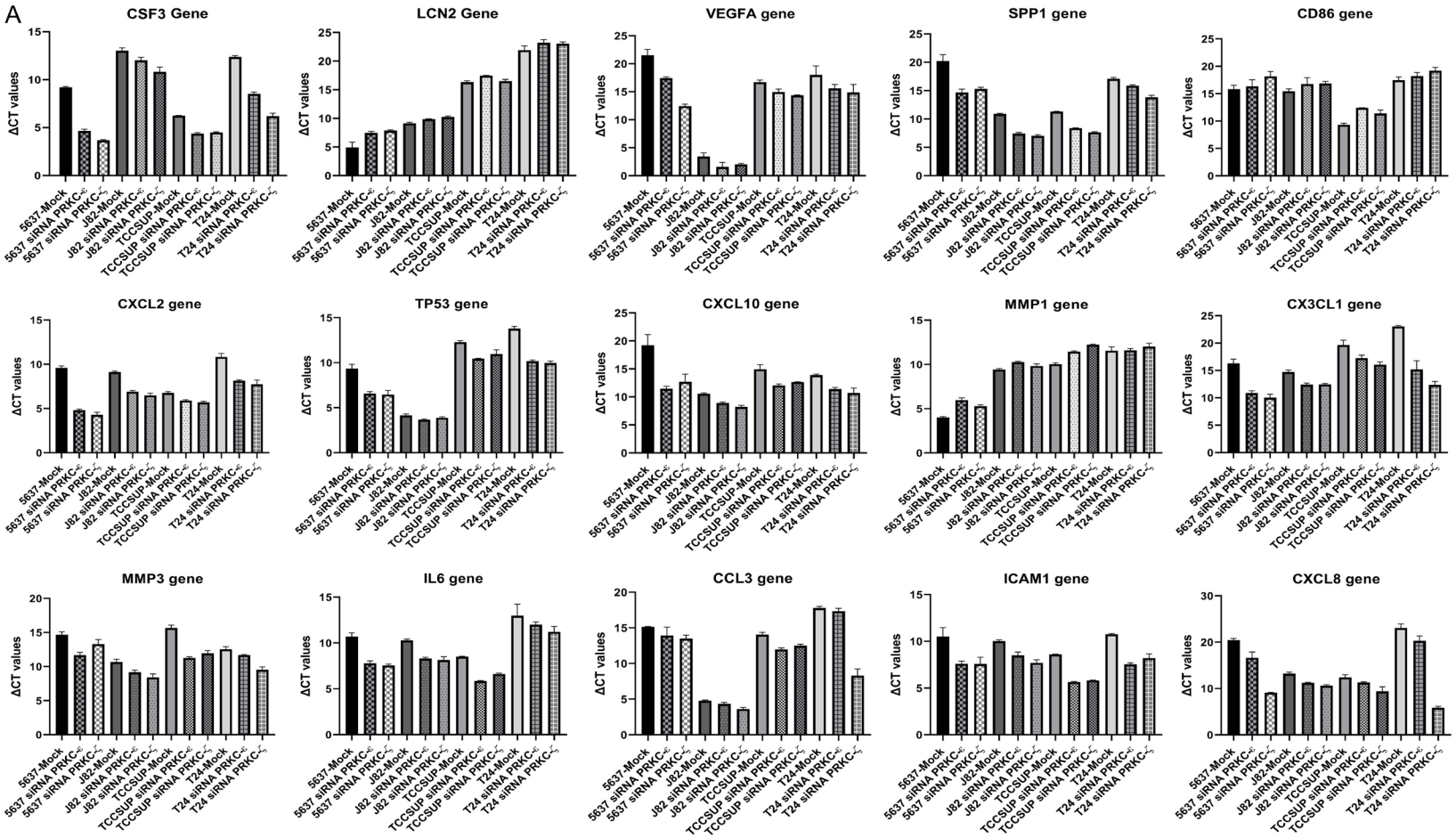
A
CSF3 Gene
LCN2 Gene
VEGFA gene
SPP1 gene
CD86 gene
CXCL2 gene
TP53 gene
CXCL10 gene
MMP1 gene
CX3CL1 gene
MMP3 gene
IL6 gene
CCL3 gene
ICAM1 gene
CXCL8 gene
ΔCT values
5637-Mock
5637 siRNA PRKCδ
5637 siRNA PRKCζ
J82-Mock
J82 siRNA PRKCδ
J82 siRNA PRKCζ
TCCSUP-Mock
TCCSUP siRNA PRKCδ
TCCSUP siRNA PRKCζ
T24-Mock
T24 siRNA PRKCδ
T24 siRNA PRKCζ

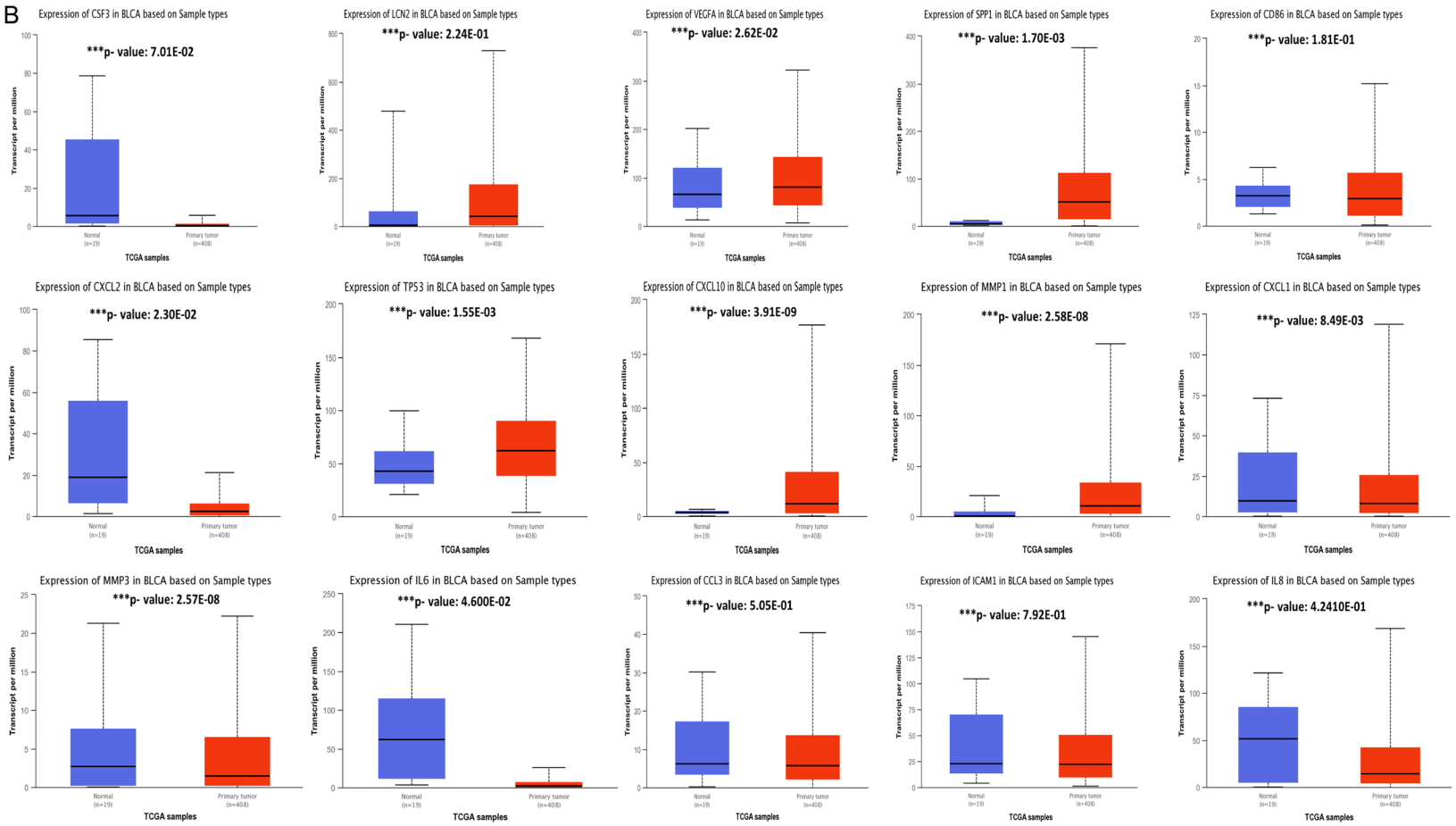
B
Expression of CSF3 in BLCA based on Sample types
***p- value: 7.01E-02
Expression of LCN2 in BLCA based on Sample types
***p- value: 2.24E-01
Expression of VEGFA in BLCA based on Sample types
***p- value: 2.62E-02
Expression of SPP1 in BLCA based on Sample types
***p- value: 1.70E-03
Expression of CD86 in BLCA based on Sample types
***p- value: 1.81E-01
Expression of CXCL2 in BLCA based on Sample types
***p- value: 2.30E-02
Expression of TP53 in BLCA based on Sample types
***p- value: 1.55E-03
Expression of CXCL10 in BLCA based on Sample types
***p- value: 3.91E-09
Expression of MMP1 in BLCA based on Sample types
***p- value: 2.58E-08
Expression of CXCL1 in BLCA based on Sample types
***p- value: 8.49E-03
Expression of MMP3 in BLCA based on Sample types
***p- value: 2.57E-08
Expression of IL6 in BLCA based on Sample types
***p- value: 4.600E-02
Expression of CCL3 in BLCA based on Sample types
***p- value: 5.05E-01
Expression of ICAM1 in BLCA based on Sample types
***p- value: 7.92E-01
Expression of IL8 in BLCA based on Sample types
***p- value: 4.2410E-01
Transcript per million
Normal (n=19)
Primary tumor (n=408)
TCGA samples

C

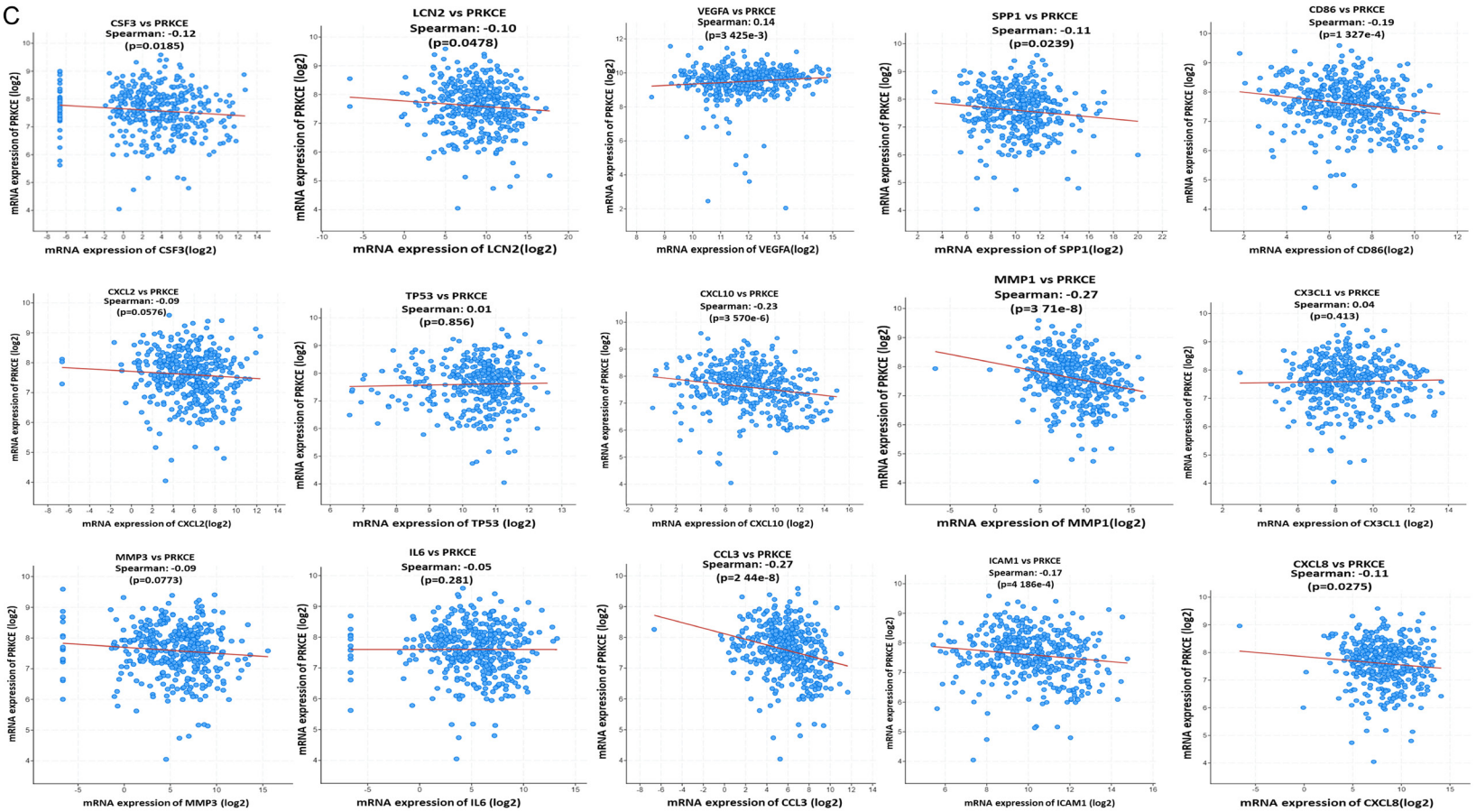
CSF3 vs PRKCE
Spearman: -0.12
(p=0.0185)
mRNA expression of CSF3(log2)
LCN2 vs PRKCE
Spearman: -0.10
(p=0.0478)
mRNA expression of LCN2(log2)
VEGFA vs PRKCE
Spearman: 0.14
(p=3 425e-3)
mRNA expression of VEGFA(log2)
SPP1 vs PRKCE
Spearman: -0.11
(p=0.0239)
mRNA expression of SPP1(log2)
CD86 vs PRKCE
Spearman: -0.19
(p=1 327e-4)
mRNA expression of CD86(log2)
CXCL2 vs PRKCE
Spearman: -0.09
(p=0.0576)
mRNA expression of CXCL2(log2)
TP53 vs PRKCE
Spearman: 0.01
(p=0.856)
mRNA expression of TP53 (log2)
CXCL10 vs PRKCE
Spearman: -0.23
(p=3 570e-6)
mRNA expression of CXCL10 (log2)
MMP1 vs PRKCE
Spearman: -0.27
(p=3 71e-8)
mRNA expression of MMP1(log2)
CX3CL1 vs PRKCE
Spearman: 0.04
(p=0.413)
mRNA expression of CX3CL1 (log2)
MMP3 vs PRKCE
Spearman: -0.09
(p=0.0773)
mRNA expression of MMP3 (log2)
IL6 vs PRKCE
Spearman: -0.05
(p=0.281)
mRNA expression of IL6 (log2)
CCL3 vs PRKCE
Spearman: -0.27
(p=2 44e-8)
mRNA expression of CCL3 (log2)
ICAM1 vs PRKCE
Spearman: -0.17
(p=4 186e-4)
mRNA expression of ICAM1 (log2)
CXCL8 vs PRKCE
Spearman: -0.11
(p=0.0275)
mRNA expression of CXCL8(log2)
mRNA expression of PRKCE (log2)

D

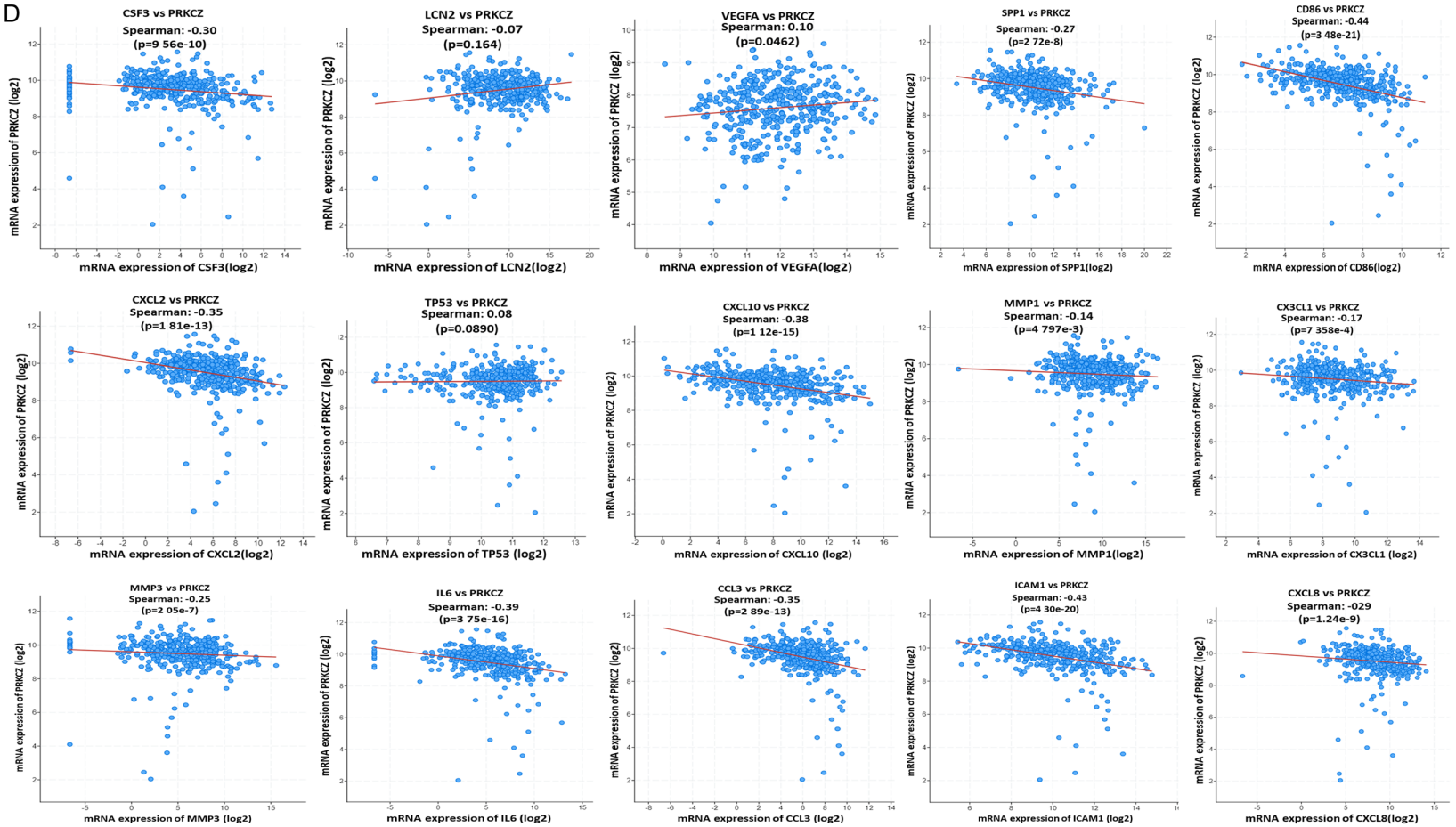
CSF3 vs PRKCZ
Spearman: -0.30
(p=9 56e-10)
mRNA expression of PRKCZ (log2)
mRNA expression of CSF3(log2)
LCN2 vs PRKCZ
Spearman: -0.07
(p=0.164)
mRNA expression of PRKCZ (log2)
mRNA expression of LCN2(log2)
VEGFA vs PRKCZ
Spearman: 0.10
(p=0.0462)
mRNA expression of PRKCZ (log2)
mRNA expression of VEGFA(log2)
SPP1 vs PRKCZ
Spearman: -0.27
(p=2 72e-8)
mRNA expression of PRKCZ (log2)
mRNA expression of SPP1(log2)
CD86 vs PRKCZ
Spearman: -0.44
(p=3 48e-21)
mRNA expression of PRKCZ (log2)
mRNA expression of CD86(log2)
CXCL2 vs PRKCZ
Spearman: -0.35
(p=1 81e-13)
mRNA expression of PRKCZ (log2)
mRNA expression of CXCL2(log2)
TP53 vs PRKCZ
Spearman: 0.08
(p=0.0890)
mRNA expression of PRKCZ (log2)
mRNA expression of TP53 (log2)
CXCL10 vs PRKCZ
Spearman: -0.38
(p=1 12e-15)
mRNA expression of PRKCZ (log2)
mRNA expression of CXCL10 (log2)
MMP1 vs PRKCZ
Spearman: -0.14
(p=4 797e-3)
mRNA expression of PRKCZ (log2)
mRNA expression of MMP1(log2)
CX3CL1 vs PRKCZ
Spearman: -0.17
(p=7 358e-4)
mRNA expression of PRKCZ (log2)
mRNA expression of CX3CL1 (log2)
MMP3 vs PRKCZ
Spearman: -0.25
(p=2 05e-7)
mRNA expression of PRKCZ (log2)
mRNA expression of MMP3 (log2)
IL6 vs PRKCZ
Spearman: -0.39
(p=3 75e-16)
mRNA expression of PRKCZ (log2)
mRNA expression of IL6 (log2)
CCL3 vs PRKCZ
Spearman: -0.35
(p=2 89e-13)
mRNA expression of PRKCZ (log2)
mRNA expression of CCL3 (log2)
ICAM1 vs PRKCZ
Spearman: -0.43
(p=4 30e-20)
mRNA expression of PRKCZ (log2)
mRNA expression of ICAM1 (log2)
CXCL8 vs PRKCZ
Spearman: -029
(p=1.24e-9)
mRNA expression of PRKCZ (log2)
mRNA expression of CXCL8(log2)

E

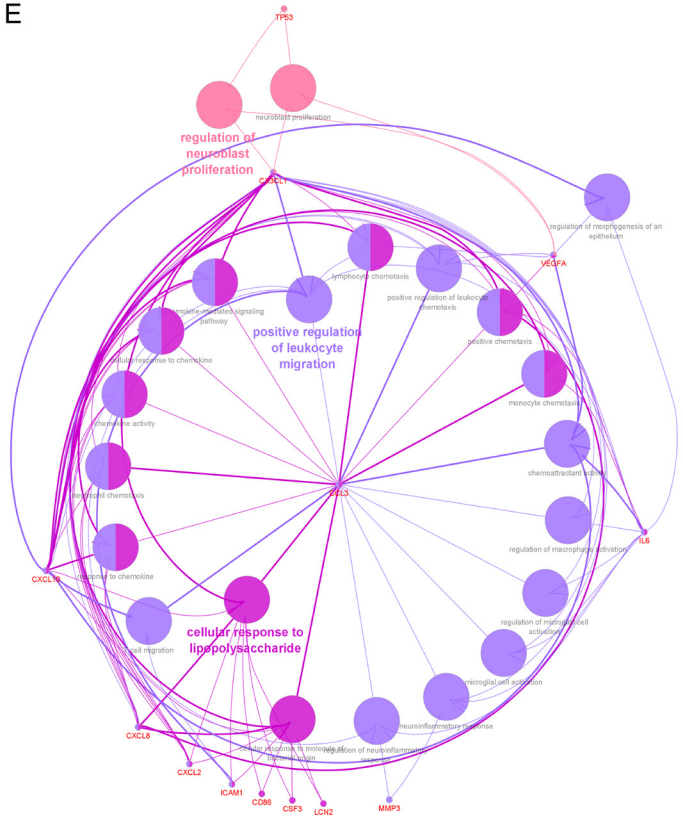
TP53
neuroblast proliferation
regulation of neuroblast proliferation
CXCL1
regulation of morphogenesis of an epithelium
VEGFA
lymphocyte chemotaxis
positive regulation of leukocyte chemotaxis
positive regulation of leukocyte migration
positive chemotaxis
monocyte chemotaxis
chemokine activity
chemoattractant activity
CCL3
IL6
regulation of macrophage activation
CXCL10
response to chemokine
cellular response to lipopolysaccharide
regulation of microglial cell activation
T cell migration
microglial cell activation
neuroinflammatory response
CXCL8
CXCL2
ICAM1
CD86
CSF3
LCN2
MMP3

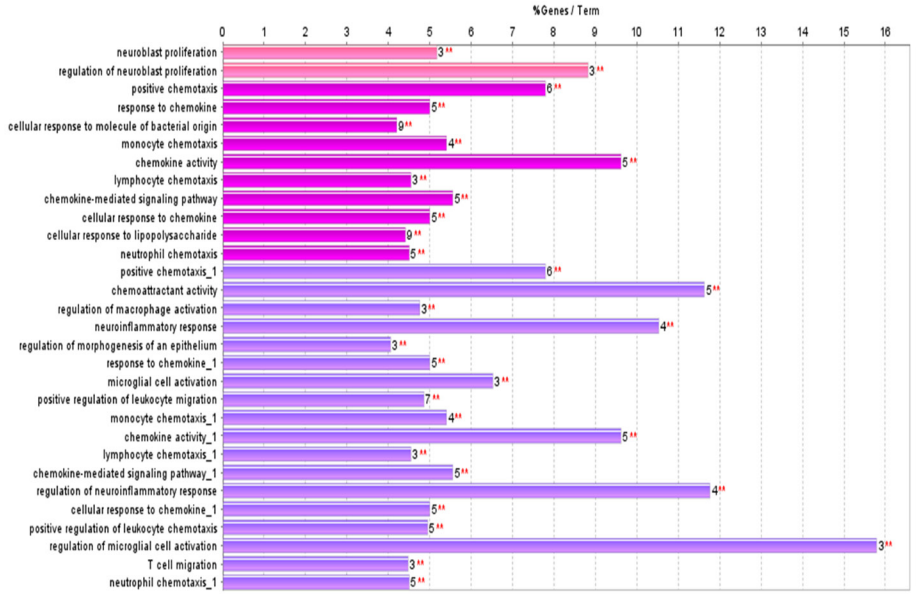
%Genes / Term
0 1 2 3 4 5 6 7 8 9 10 11 12 13 14 15 16
neuroblast proliferation 3**
regulation of neuroblast proliferation 3**
positive chemotaxis 6**
response to chemokine 5**
cellular response to molecule of bacterial origin 9**
monocyte chemotaxis 4**
chemokine activity 5**
lymphocyte chemotaxis 3**
chemokine-mediated signaling pathway 5**
cellular response to chemokine 5**
cellular response to lipopolysaccharide 9**
neutrophil chemotaxis 5**
positive chemotaxis_1 6**
chemoattractant activity 5**
regulation of macrophage activation 3**
neuroinflammatory response 4**
regulation of morphogenesis of an epithelium 3**
response to chemokine_1 5**
microglial cell activation 3**
positive regulation of leukocyte migration 7**
monocyte chemotaxis_1 4**
chemokine activity_1 5**
lymphocyte chemotaxis_1 3**
chemokine-mediated signaling pathway_1 5**
regulation of neuroinflammatory response 4**
cellular response to chemokine_1 5**
positive regulation of leukocyte chemotaxis 5**
regulation of microglial cell activation 3**
T cell migration 3**
neutrophil chemotaxis_1 5**

F

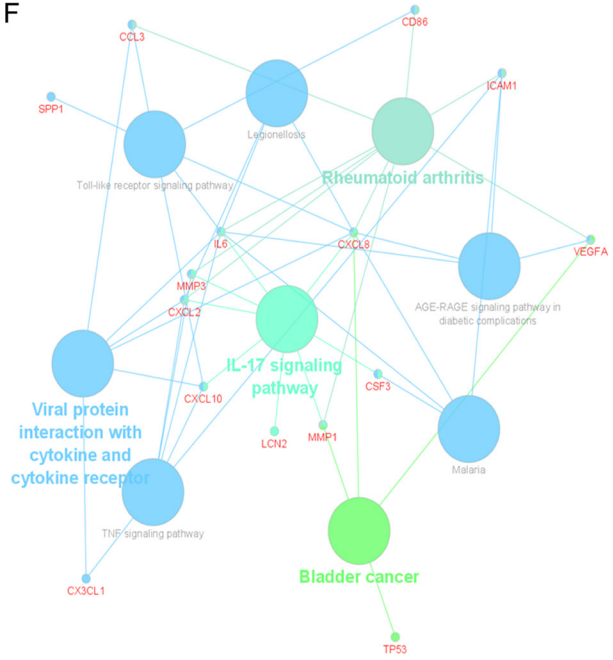
CCL3
CD86
SPP1
ICAM1
Legionellosis
Toll-like receptor signaling pathway
Rheumatoid arthritis
IL6
CXCL8
VEGFA
MMP3
CXCL2
AGE-RAGE signaling pathway in diabetic complications
IL-17 signaling pathway
CSF3
CXCL10
Viral protein interaction with cytokine and cytokine receptor
LCN2
MMP1
Malaria
TNF signaling pathway
Bladder cancer
CX3CL1
TP53

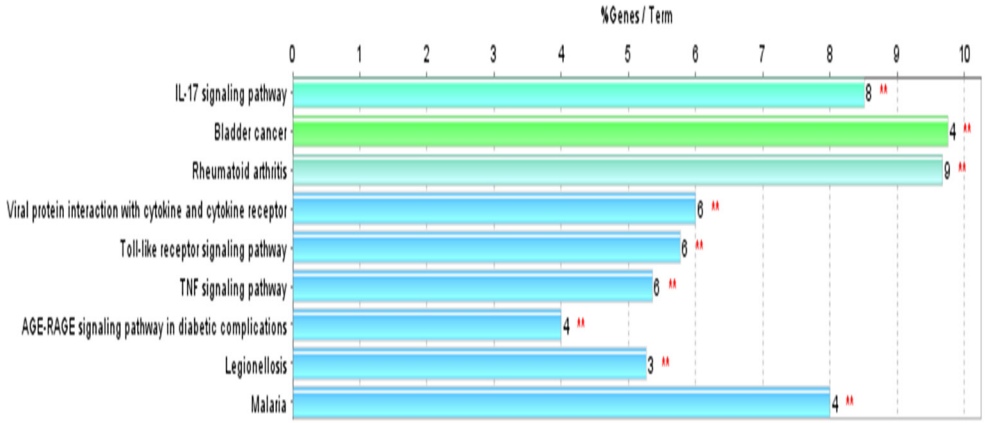
%Genes / Term
0
1
2
3
4
5
6
7
8
9
10
IL-17 signaling pathway
8
Bladder cancer
4
Rheumatoid arthritis
9
Viral protein interaction with cytokine and cytokine receptor
6
Toll-like receptor signaling pathway
6
TNF signaling pathway
6
AGE-RAGE signaling pathway in diabetic complications
4
Legionellosis
3
Malaria
4

G

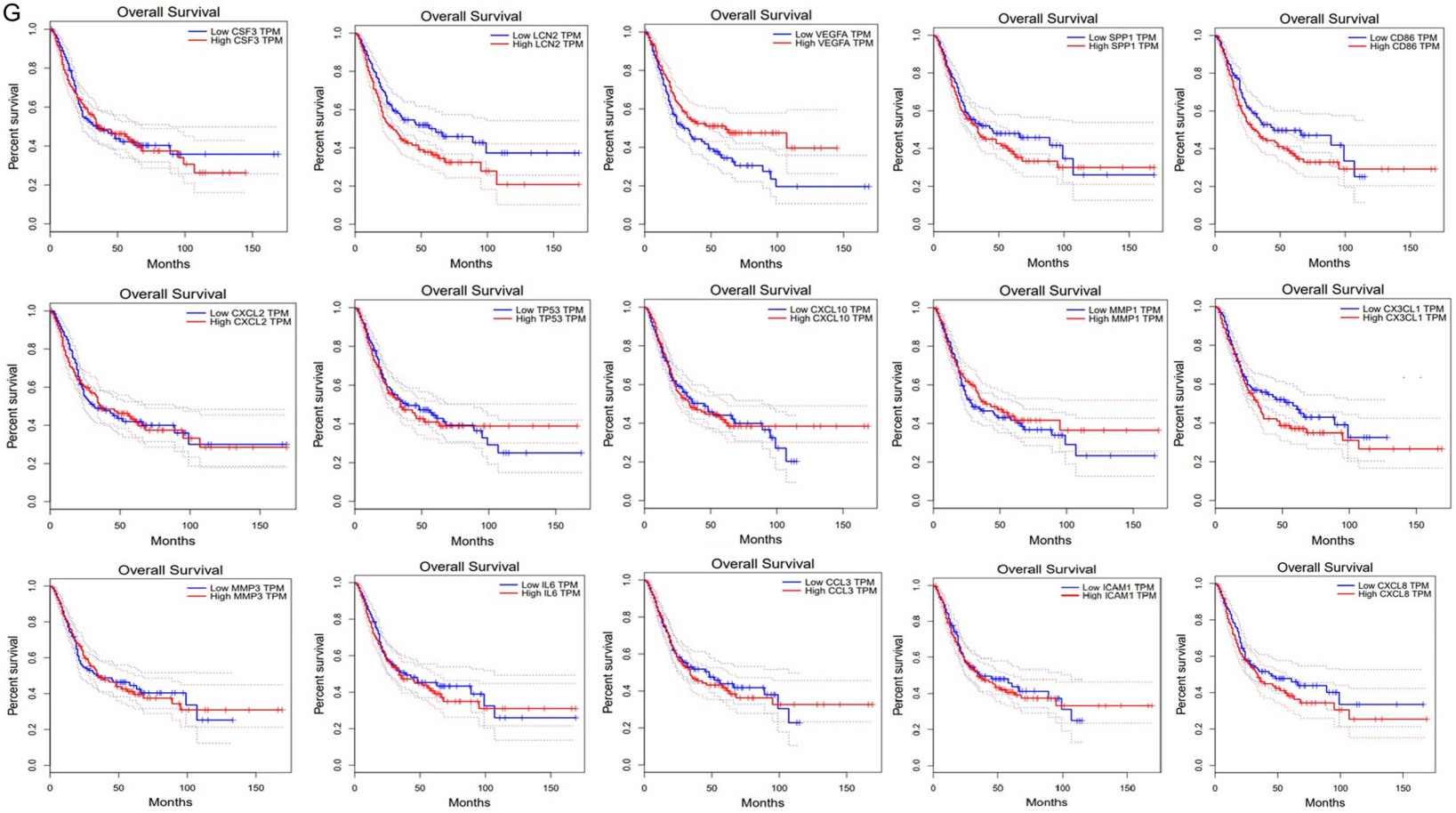
Overall Survival
Low CSF3 TPM
High CSF3 TPM
Low LCN2 TPM
High LCN2 TPM
Low VEGFA TPM
High VEGFA TPM
Low SPP1 TPM
High SPP1 TPM
Low CD86 TPM
High CD86 TPM
Low CXCL2 TPM
High CXCL2 TPM
Low TP53 TPM
High TP53 TPM
Low CXCL10 TPM
High CXCL10 TPM
Low MMP1 TPM
High MMP1 TPM
Low CX3CL1 TPM
High CX3CL1 TPM
Low MMP3 TPM
High MMP3 TPM
Low IL6 TPM
High IL6 TPM
Low CCL3 TPM
High CCL3 TPM
Low ICAM1 TPM
High ICAM1 TPM
Low CXCL8 TPM
High CXCL8 TPM
Percent survival
Months

H

CXCL8

HPA057179
Patient id: 3465
Tumor cells
Staining: not detected
Intensity: **Weak**
Quality: <25%
Location: cytoplasmic/ membrane

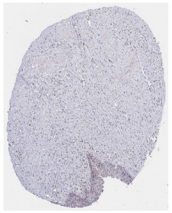

Urinary bladder

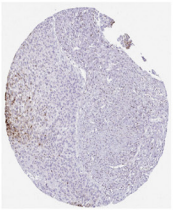

Urinary bladder carcinoma

HPA057179
Patient id: 3517
Tumor cells
Staining: not detected
Intensity: **Weak**
Quality: <25%
Location: cytoplasmic/ membrane

TP53

CAB039239
Patient id: 1798
Tumor cells
Staining: not detected
Intensity: **Negative**
Location: none

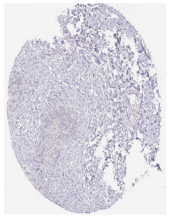

Urinary bladder

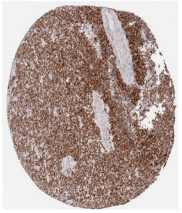

Urinary bladder carcinoma

CAB039239
Patient id: 3112
Tumor cells
Staining: **High**
Intensity: Strong
Quality: >75%
Location: cytoplasmic/ membrane

SPP1

HPA027541
Patient id: 3543
Tumor cells
Staining: **Low**
Intensity: **weak**
Quality: <25%
Location: cytoplasmic/ membrane

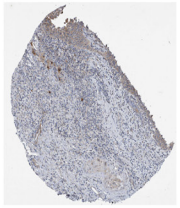

Urinary bladder

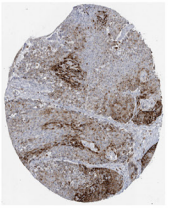

Urinary bladder carcinoma

HPA027541
Patient id: 3516
Tumor cells
Staining: **High**
Intensity: **Strong**
Quality: 75-25%
Location: cytoplasmic/ membrane

MMP3

HPA007875
Patient id: 1921
Urothelial cells
Staining: **High**
Intensity: Strong
Quality: >75%
Location: cytoplasmic/ membrane

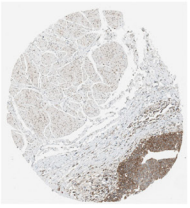

Urinary bladder

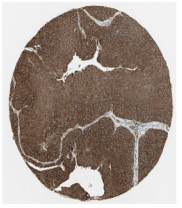

Urinary bladder carcinoma

HPA007875
Patient id: 1774
Tumor cells
Staining: **High**
Intensity: Strong
Quality: >75%
Location: cytoplasmic/ membrane

VEGFA

CAB039240
Patient id: 1798
Urothelial cells
Staining: High
Intensity: Strong
Quality: 75-25%
Location: cytoplasmic/ membrane

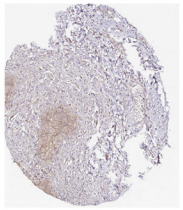

Urinary bladder

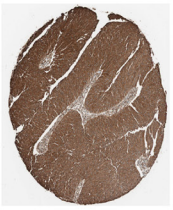

Urinary bladder carcinoma

CAB005429
Patient id: 3265
Tumor cells
Staining: **High**
Intensity: Strong
Quality: >75%
Location: cytoplasmic/ membrane

ICAM1

HPA057179
Patient id: 3465
Tumor cells
Staining: not detected
Intensity: **Negative**
Location: none

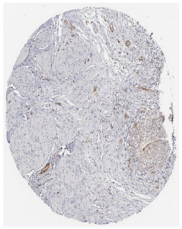

Urinary bladder

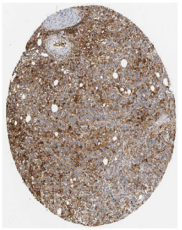

Urinary bladder carcinoma

HPA004877
Patient id: 1984
Tumor cells
Staining: **High**
Intensity: Strong
Quality: >75%
Location: cytoplasmic/ membrane

CXCL10

HPA045942
Patient id: 2470
Tumor cells
Staining: not detected
Intensity: **Negative**
Location: none

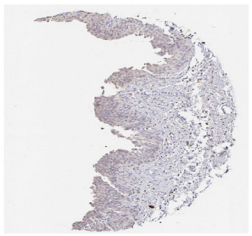

Urinary bladder

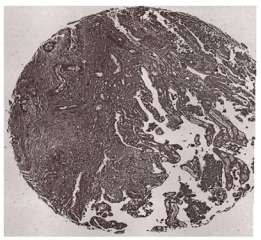

Urinary bladder carcinoma

Stage:IIIA
pTNM: T4aN0M0
Staining: High
Intensity: strong
Quality: 75-85%
Location: cytoplasmic/ membrane
NBP3-11846 - Human Bladder Tissue MicroArray (Cancer)

Figure 3. Hub gene dysregulation and biological variance. A. mRNA expression of 15 hub genes in response to PRKC-ε & ζ silencing among different grade of bladder cancer cell (5637, J82, TCCSUP and T24); non-transfected cells are taken as controls. B. Expression of hub genes in Urothelial Bladder cancer vs normal Bladder tissue from TCGA data. Statistical significance has been indicated in the figures, ***P < 0.001. C, D. Correlation analysis of hub genes with Protein kinase C-ε & ζ with a Spearman correlation scatter plot with regression line (red line) depicting a statistically significant co-relationship of hub genes with the kinase. The negative value of Spearman indicates an inverse co-relationship between the kinase and the hub genes. E, F. The image represents the functional enrichment analysis under GO KEGG pathway. Gene annotations are in terms of the percentage of gene/term for represented Module. G. Cox multivariate proportional hazard model curves for overall survival of the hub genes obtained from bladder cancer survival database. The two line shows high (red) and low (blue) percentage of the genes in respect to the time interval (months), n = 201. H. Immunohistochemical analysis of the hub genes. The protein expression of identified hub genes (CXCL8, SPP1, VEGFA, TP53, MMP3 and ICAM1) was assessed in Bladder cancer tissues and normal urothelial bladder tissue derived from Human Protein Atlas database and the expression of CXCL10 was assessed through Tissue microarray (NBP3-11846 - Human Bladder Tissue MicroArray Cancer).

Table 3. Hub genes expression in study and TCGA data and association with survival

S.No	*ID*	*Cox p-value*	*HR (Hazard Ratio)*	*Dataset*	*Probe ID*	*Cohort*	*mRNA expression (TCGA)*	*Experimental data (siRNA knockdown) expression*
1.	CSF3	0.34	1.58	GSE13507	ILMN_1706852	CNUH	downregulated	downregulated
2.	LCN2	0.42	0.91	GSE13507	ILMN_1692223	CNUH	upregulated	upregulated
3.	VEGFA	0.80	0.94	GSE5287	210512_s_at	Aarhus (1995-2004)	upregulated	downregulated
4.	SPP1	0.18	1.11	GSE13507	ILMN_1651354	CNUH	upregulated	downregulated
5.	CD86	0.64	1.15	GSE13507	ILMN_1714602	CNUH	upregulated	upregulated
6.	CXCL2	0.61	1.07	GSE13507	ILMN_1682636	CNUH	downregulated	downregulated
7.	TP53	0.00	0.43	GSE5287	201746_s_at	Aarhus (1995-2004)	upregulated	downregulated
8.	CXCL10	0.09	0.96	GSE13507	ILMN_1791759	CNUH	upregulated	downregulated
9.	MMP1	0.27	1.07	GSE13507	ILMN_1726448	CNUH	upregulated	upregulated
10.	CX3CL1	0.38	0.92	GSE13507	ILMN_1654072	CNUH	downregulated	downregulated
11.	MMP3	0.57	0.92	GSE13507	ILMN_1784459	CNUH	upregulated	downregulated
12.	IL6	0.16	1.18	GSE13507	ILMN_1699651	CNUH	downregulated	downregulated
13.	CCL3	0.05	1.42	GSE13507	ILMN_1724449	CNUH	downregulated	downregulated
14.	ICAM1	0.07	1.36	GSE13507	ILMN_1812226	CNUH	upregulated	downregulated
15.	CXCL8	0.47	1.22	GSE5287	202638_s_at	Aarhus (1995-2004)	upregulated	downregulated

expression (**Table 3**) indicates that genes CXCL8, CXCL10, SPP1, VEGFA, TP53, MMP3 and ICAM1 are hub genes which have statistically significant downregulated mRNA expression in different grades of bladder cancer cells due to kinase inhibition. Upon TCGA database analysis their expression was found to be upregulated in BLCA. Upon correlation analysis, these genes show statistical significance with both the isozymes, and have significant role in bladder cancer.

Discussion

Protein kinase C (PRKC) transfers phosphoryl groups onto target proteins, thereby altering their activity and regulating signalling pathways. They are reported as tumor promoters and contribute to oncogenesis [17, 18]. Despite the distinct intracellular location and differential access to substrates, PRKC isozymes show impressive functional selectivity in cells with high homology and similar substrate specificity in vitro [19]. The effect of PRKC-α inhibition in epithelial cancers has been studied [20]; however, the overall profile of genes and signalling pathways involved in the suppression of carcinogenic characteristics with the ε & ζ isozymes has not been reported yet. Therefore, in this study, we evaluated the effect of the knockdown of PRKC ε & ζ isozymes in combination on bladder cancer tumorigenesis. Our analysis shows a statistically significant downregulatory effect on the expression of 15 hub genes with a strong association of differentially regulated pathways relevant for controlling the immune response, inflammation, proliferation, differentiation, apoptosis, and angiogenesis. The identified genes were further validated in control (non-transfected) and knockdown samples via

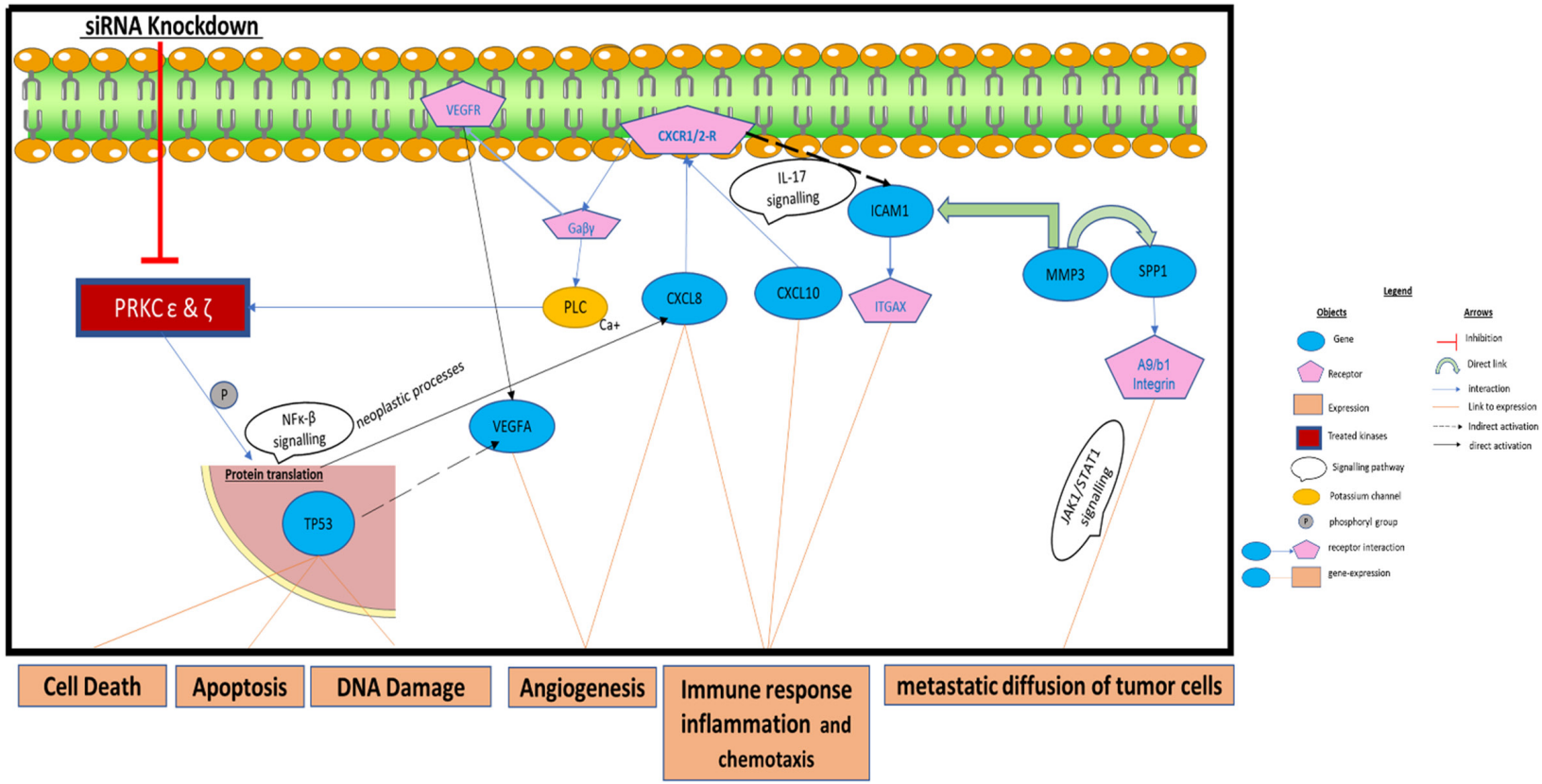

Figure 4. Masking of kinase activity revealed potential genes associated with PRKC ε & ζ tumorigenesis in bladder cancer cells.

qRT-PCR and Bladder cancer datasets of TCGA. Upon evaluating the mRNA expression of hub genes in PRKC-ε & ζ knockdown samples, it was found that the hub genes were regulated by both the kinases in all the four grades of bladder cancer cells (5637, J82, TCCSUP, T24). Among these only 7 genes TP53, CXCL8, CXCL10, MMP3, SPP1, VEGFA and ICAM1 were identified to be directly associated with bladder cancer progression and tumorigenesis (**Figure 4**). Further analysis revealed that these genes were primarily enriched in hallmark gene sets such as inflammatory response (M5932), TNF-α signalling via NFK-β interaction (M5890), Epithelial Mesenchymal Transition (M5930), cytokine-cytokine receptor interaction (hsa04060), and IL-17 signalling (hsa04657) and display statistical significance for survival in bladder cancer.

The initiation of an appropriate microenvironment of tumor mediated immune response requires chemokine-receptors expressed on tumor cells [21]. These receptors enhance the chemokines activity, which may lead to invasiveness and evoke a cascade of changes leading to epithelial to mesenchymal transition [22, 23]. In this study, two inflammatory chemokines CXCL10 and CXCL8 were downregulated by both PRKC-ε & ζ isozymes. The increased levels of these cytokines are associated with leukocyte homing to inflamed tissues, which exacerbates inflammation and significantly damages tissue [24]. These chemokines are secreted by different cell types, including lymphocytes, neutrophils, macrophages, and many tumor cells [25, 26]. Many advanced human malignancies, such as ovarian carcinoma, multiple myeloma and B-cell lymphoma, have also been linked to elevated expression of CXCL10 [27-29]. It is also correlated with poor survival in patients with ovarian cancer and colon cancer [30, 31]. Similarly, the binding of CXCL8 to the CXCR1 and CXCR2 cell-surface G protein-coupled receptors allows inflammation which induces Protein Kinase C (PRKC), Akt/PKB, and MAPK signalling [32]. CXCL8 enhances the neutrophil chemoattractant protein, which further increases the infiltrating monocytes and lymphocytes in the tumor microenvironment (TME) [33]. This property of CXCL8 allows it to play a key role in tumor progression by enhancing the proliferation, invasion, and angiogenesis of tumors [34]. Many studies have projected CXCL8 as a urinary biomarker in bladder cancer [35].

Another crucial protein which acts as a ligand for the leukocyte adhesion protein LFA-1 (integrin alpha-L/beta-2) and has a critical role in cell adhesion, leucocyte trans endothelial migration to areas of inflammation, and lymphocyte activation [33] is ICAM-1. The affinity and clustering of LFA-1 rise when leukocytes are triggered by any of several exogenous stimuli, such as chemokines [36]. It is observed in prostate tumor cells, ICAM-1 and TGFβ2 signalling caused perforin to be downregulated via MMP's interactions which caused invasion [37]. Similarly, in our data analysis, it was found that MMP3 displays interaction with the ICAM1 via Epithelial Mesenchymal Transition (map04520) in bladder cancer.

Another hallmark of tumor progression includes mutation of the tumor suppressor gene TP53, which results in an increased risk of bladder cancer development [38]. Mutations in p53 influence cytokine signalling via NF-κB mediated transcriptional activation of CXC chemokines. The enhancement in pro-inflammatory signal results in the activation of transcription, apoptosis, and altered cell cycle events [39]. Previous research revealed that TP53 function was inactivated in 76% of muscle invasive bladder cancer (MIBC) and 50% of MIBC samples had TP53 mutations [40]. The mutation in "TP53" called as driver mutation in bladder cancer affect response to cancer chemotherapy and drug susceptibility, hence lead to poorer prognosis [41]. These mutations are reported for neoplastic processes, tumor vascularization and metastatic spread of tumor via regulating vascular endothelial growth factor (VEGF-A), which is reported to be the most significant angiogenic regulator [42]. Its overexpression in pre-chemotherapy samples was found to be a strong predictor of recurrence and death in locally advanced urothelial cancer undergoing cystectomy and chemotherapy [43]. Also, the higher levels of VEGF in tumor tissue led to progression in bladder transitional cell carcinoma (TCC), and increased urinary levels act as a marker for recurrence in patients with superficial lesions [44, 45]. This proangiogenic factor is regulated by MMPs [46], which are responsible for SPP1 upregulation and stimulate the JAK1/STAT1 signalling pathway. This, in res-

ponse, increases proliferation and invasion and prevents apoptosis [47]. Recent studies revealed that SPP1 expression is correlated with the development of tumors in the breast, lung, prostate, liver, stomach, colon, cervix, and ovary and that the plasma concentration of SPP1 in patients with metastatic disease is significantly higher than that of normal serum [48, 49]. The kinase inhibition downregulated the expression of all the 7 genes, and may be beneficial to target tumorigenesis.

The current analysis has uncovered the PRKC interaction and modulation of oncogenes and tumor suppressor genes. Protein Kinase C signalling has come out to be vital for the regulation of events that are important for tumor progression via cytokines interaction, adhesion molecules such as ICAM, VEGFA, SPP1 and MMP3 along with mutated oncogene TP53 for regulation of cell death. All the identified hub genes modulate the cell cycle control, DNA damage, angiogenesis, immune response, and apoptosis. The current study shows that the functionality of PRKC isozymes, ε & ζ, drive the tumorigenic phenotypes in bladder cancer. Further studies may establish the role of PRKC inhibitors, based on cell selectivity and toxicity in bladder cancer treatment by *in vivo* studies.

Acknowledgements

The work is supported by ad-hoc research grant to Usha Agrawal (UA), Indian Council of Medical Research (ICMR) (Grant No. 5/13/37/2014/NCD-III).

Disclosure of conflict of interest

None.

Abbreviations

PRKC, Protein kinase C; TKI's, tyrosine kinase inhibitors; BC, Bladder carcinoma; DEGs, Differentially expressed genes; TCC, Transitional cell carcinoma; MIBC, muscle invasive bladder cancer; MMP, Matrix metalloproteins; VEGFA, Vascular endothelial growth factors; ICAM, Intracellular adhesion molecule; SPP1, Secreted Phosphoprotein 1; CXCL8, C-X-C Motif Chemokine Ligand 8; SDS-PAGE, Sodium Dodecyl Sulphate-Polyacrylamide Gel Electrophoresis; RIN, RNA integrity number; FDR, false discovery rate; GO, gene ontology; KEGG, Kyoto Encyclopaedia of Genes and Genomes; BLCA, Bladder cancer datasets; Tukey HSD, honest significant difference.

Address correspondence to: Usha Agrawal, ICMR-National Institute of Pathology, New Delhi, India. ORCID: 0000-0001-7539-4102; E-mail: ushakaggarwal.nip@gov.in

References

[1] Antal CE, Hudson AM, Kang E, Zanca C, Wirth C, Stephenson NL, Trotter EW, Gallegos LL, Miller CJ, Furnari FB, Hunter T, Brognard J and Newton AC. Cancer-associated protein kinase C mutations reveal kinase's role as tumor suppressor. Cell 2015; 160: 489-502.

[2] D'Amico AE and Lennartz MR. Protein kinase C-epsilon in membrane delivery during phagocytosis. J Immunol Sci 2018; 2: 26-32.

[3] Steinberg SF. Structural basis of protein kinase C isoform function. Physiol Rev 2008; 88: 1341-1378.

[4] Nasa I and Kettenbach AN. Coordination of protein kinase and phosphoprotein phosphatase activities in mitosis. Front Cell Dev Biol 2018; 6: 30.

[5] Kannaiyan R and Mahadevan D. A comprehensive review of protein kinase inhibitors for cancer therapy. Expert Rev Anticancer Ther 2018; 18: 1249-1270.

[6] He S, Li Q, Huang Q and Cheng J. Targeting protein kinase C for cancer therapy. Cancers (Basel) 2022; 14: 1104.

[7] Demkova L and Kucerova L. Role of the HGF/c-MET tyrosine kinase inhibitors in metastasic melanoma. Mol Cancer 2018; 17: 26.

[8] Kudo Y, Sugimoto M, Arias E, Kasashima H, Cordes T, Linares JF, Duran A, Nakanishi Y, Nakanishi N, L'Hermitte A, Campos A, Senni N, Rooslid T, Roberts LR, Cuervo AM, Metallo CM, Karin M, Diaz-Meco MT and Moscat J. PKClambda/iota loss induces autophagy, oxidative phosphorylation, and NRF2 to promote liver cancer progression. Cancer Cell 2020; 38: 247-262, e11.

[9] Jiang T, Xia Y, Lv J, Li B, Li Y, Wang S, Xuan Z, Xie L, Qiu S, He Z, Wang L and Xu Z. A novel protein encoded by circMAPK1 inhibits progression of gastric cancer by suppressing activation of MAPK signaling. Mol Cancer 2021; 20: 66.

[10] Kawano T, Inokuchi J, Eto M, Murata M and Kang JH. Protein kinase C (PKC) isozymes as diagnostic and prognostic biomarkers and therapeutic targets for cancer. Cancers (Basel) 2022; 14: 5425.

[11] Parker PJ, Lockwood N, Davis K, Kelly JR, Soliman TN, Pardo AL, Marshall JJT, Redmond JM, Vitale M and Silvia Martini. A cancer-associat-

ed, genome protective programme engaging PKCε. Adv Biol Regul 2020; 78: 100759.
[12] Zang G, Mu Y, Gao L, Bergh A and Landstrom M. PKCζ facilitates lymphatic metastatic spread of prostate cancer cells in a mice xenograft model. Oncogene 2019; 38: 4215-4231.
[13] Pears C, Schaap D and Parker PJ. The regulatory domain of protein kinase C-epsilon restricts the catalytic-domain-specificity. Biochem J 1991; 276: 257-260.
[14] Alassaf E and Mueller A. The role of PKC in CXCL8 and CXCL10 directed prostate, breast and leukemic cancer cell migration. Eur J Pharmacol 2020; 886: 173453.
[15] Kawano T, Inokuchi J, Eto M, Murata M and Kang JH. Activators and inhibitors of protein kinase C (PKC): their applications in clinical trials. Pharmaceutics 2021; 13: 1748.
[16] Cortes JE, Muresan B, Mamolo C, Cappelleri JC, Crescenzo RJ, Su Y, Gambacorti-Passerini C, Heeg B and Douglas Smith B. Matching-adjusted indirect comparison of bosutinib, dasatinib and nilotinib effect on survival and major cytogenetic response in treatment of second-line chronic phase chronic myeloid leukemia. Curr Med Res Opin 2019; 35: 1615-1622.
[17] Hallal M, Braga-Lagache S, Jankovic J, Simillion C, Bruggmann R, Uldry AC, Allam R, Heller M and Bonadies N. Inference of kinase-signaling networks in human myeloid cell line models by Phosphoproteomics using kinase activity enrichment analysis (KAEA). BMC Cancer 2021; 21: 789.
[18] Lei Z, Wang J, Sun W, Chen X, Jiao W, Zhang H, Lei T and Li F. PKCdelta reveals a tumor promoter function by promoting cell proliferation and migration in somatotropinomas. Int J Clin Exp Pathol 2018; 11: 208-215.
[19] Casado-Medrano V, Baker MJ, Cooke M and Kazanietz MG. Mechanisms of protein kinase C epsilon down-regulation by transforming growth factor-beta in lung cancer cells. bioRxiv 2020; [Epub ahead of print].
[20] Black AR and Black JD. The complexities of PKCalpha signaling in cancer. Adv Biol Regul 2021; 80: 100769.
[21] Bule P, Aguiar SI, Aires-Da-Silva F and Dias JNR. Chemokine-directed tumor microenvironment modulation in cancer immunotherapy. Int J Mol Sci 2021; 22: 9804.
[22] Ribatti D, Tamma R and Annese T. Epithelial-mesenchymal transition in cancer: a historical overview. Transl Oncol 2020; 13: 100773.
[23] Zhang R, Li Y, Pan B, Li Y, Liu A and Li X. Increased expression of hub gene CXCL10 in peripheral blood mononuclear cells of patients with systemic lupus erythematosus. Exp Ther Med 2019; 18: 4067-4075.
[24] Metzemaekers M, Vanheule V, Janssens R, Struyf S and Proost P. Overview of the mechanisms that may contribute to the non-redundant activities of interferon-inducible CXC chemokine receptor 3 ligands. Front Immunol 2018; 8: 1970.
[25] Zirlik K and Duyster J. Anti-angiogenics: current situation and future perspectives. Oncol Res Treat 2018; 41: 166-171.
[26] Situ Y, Lu X, Cui Y, Xu Q, Deng L, Lin H, Shao Z and Chen J. Systematic analysis of CXC chemokine-vascular endothelial growth factor A network in colonic adenocarcinoma from the perspective of angiogenesis. Biomed Res Int 2022; 2022: 5137301.
[27] Ignacio RMC, Lee ES, Wilson AJ, Beeghly-Fadiel A, Whalen MM and Son DS. Chemokine network and overall survival in TP53 wild-type and mutant ovarian cancer. Immune Netw 2018; 18: e29.
[28] Bonanni V, Antonangeli F, Santoni A and Bernardini G. Targeting of CXCR3 improves anti-myeloma efficacy of adoptively transferred activated natural killer cells. J Immunother Cancer 2019; 7: 290.
[29] Manukyan G, Papajik T, Mikulkova Z, Urbanova R, Kraiczova VS, Savara J, Kudelka M, Turcsanyi P and Kriegova E. High CXCR3 on leukemic cells distinguishes IgHV^{mut} from IgHV^{unmut} in chronic lymphocytic leukemia: evidence from CD5^{high} and CD5^{low} clones. J Immunol Res 2020; 2020: 7084268.
[30] Jin J, Li Y, Muluh TA, Zhi L and Zhao Q. Identification of CXCL10-relevant tumor microenvironment characterization and clinical outcome in ovarian cancer. Front Genet 2021; 12: 678747.
[31] Chen J, Chen QL, Wang WH, Chen XL, Hu XQ, Liang ZQ, Cao YB, Cao YM and Su SB. Prognostic and predictive values of CXCL10 in colorectal cancer. Clin Transl Oncol 2020; 22: 1548-1564.
[32] Guo Y, Zang Y, Lv L, Cai F, Qian T, Zhang G and Feng Q. IL-8 promotes proliferation and inhibition of apoptosis via STAT3/AKT/NF-κB pathway in prostate cancer. Mol Med Rep 2017; 16: 9035-9042.
[33] Walling BL and Kim M. LFA-1 in T cell migration and differentiation. Front Immunol 2018; 9: 952.
[34] Filippi MD. Neutrophil transendothelial migration: updates and new perspectives. Blood 2019; 133: 2149-2158.
[35] Ferro M, La Civita E, Liotti A, Cennamo M, Tortora F, Buonerba C, Crocetto F, Lucarelli G, Busetto GM, Del Giudice F, de Cobelli O, Carrieri G, Porreca A, Cimmino A and Terracciano D. Liquid biopsy biomarkers in urine: a route towards molecular diagnosis and personalized

medicine of bladder cancer. J Pers Med 2021; 11: 237.
[36] Zimmerman T and Blanco FJ. Inhibitors targeting the LFA-1/ICAM-1 cell-adhesion interaction: design and mechanism of action. Curr Pharm Des 2008; 14: 2128-2139.
[37] Hartana CA, Ahlen Bergman E, Zirakzadeh AA, Krantz D, Winerdal ME, Winerdal M, Johansson M, Alamdari F, Jakubczyk T, Glise H, Riklund K, Sherif A and Winqvist O. Urothelial bladder cancer may suppress perforin expression in CD8+ T cells by an ICAM-1/TGFbeta2 mediated pathway. PLoS One 2018; 13: e0200079.
[38] Lavallee E, Sfakianos JP and Mulholland DJ. Tumor heterogeneity and consequences for bladder cancer treatment. Cancers (Basel) 2021; 13: 5297.
[39] Sullivan KD, Galbraith MD, Andrysik Z and Espinosa JM. Mechanisms of transcriptional regulation by p53. Cell Death Differ 2018; 25: 133-143.
[40] Li Y, Sun L, Guo X, Mo N, Zhang J and Li C. Frontiers in bladder cancer genomic research. Front Oncol 2021; 11: 670729.
[41] Wu G, Wang F, Li K, Li S, Zhao C, Fan C and Wang J. Significance of TP53 mutation in bladder cancer disease progression and drug selection. PeerJ 2019; 7: e8261.
[42] Sadaf A, Rahman MZ, Bhattacharjee P, Ahamad MSU and Nasreen S. Significance of vascular endothelial growth factor expression in the bladder urothelial carcinoma and its association with tumor grade and invasiveness. Iran J Pathol 2021; 16: 362-369.
[43] Narayanan S and Srinivas S. Incorporating VEGF-targeted therapy in advanced urothelial cancer. Ther Adv Med Oncol 2017; 9: 33-45.
[44] Sankhwar M, Sankhwar SN, Abhishek A and Rajender S. Clinical significance of the VEGF level in urinary bladder carcinoma. Cancer Biomark 2015; 15: 349-355.
[45] Melincovici CS, Bosca AB, Susman S, Marginean M, Mihu C, Istrate M, Moldovan IM, Roman AL and Mihu CM. Vascular endothelial growth factor (VEGF) - key factor in normal and pathological angiogenesis. Rom J Morphol Embryol 2018; 59: 455-467.
[46] Fan D and Kassiri Z. Biology of tissue inhibitor of metalloproteinase 3 (TIMP3), and its therapeutic implications in cardiovascular pathology. Front Physiol 2020; 11: 661.
[47] Wang M, Sun X, Xin H, Wen Z and Cheng Y. SPP1 promotes radiation resistance through JAK2/STAT3 pathway in esophageal carcinoma. Cancer Med 2022; 11: 4526-4543.
[48] Tu Y, Chen C and Fan G. Association between the expression of secreted phosphoprotein - related genes and prognosis of human cancer. BMC Cancer 2019; 19: 1230.
[49] Li Y, He S, He A, Guan B, Ge G, Zhan Y, Wu Y, Gong Y, Peng D, Bao Z, Li X and Zhou L. Identification of plasma secreted phosphoprotein 1 as a novel biomarker for upper tract urothelial carcinomas. Biomed Pharmacother 2019; 113: 108744.
[50] Szklarczyk D, Gable AL, Nastou KC, Lyon D, Kirsch R, Pyysalo S, Doncheva NT, Legeay M, Fang T, Bork P, Jensen LJ and von Mering C. The STRING database in 2021: customizable protein-protein networks, and functional characterization of user-uploaded gene/measurement sets. Nucleic Acids Res 2021; 49: D605-D612.
[51] Adesso G, Datta N, Hall MJ and Sagawa T. Corrigendum: Shannon's information theory 70 years on: applications in classical and quantum physics. J Phys A Math Theor 2019; 52: 479501.
[52] Wang G, Oh DH and Dassanayake M. GOMCL: a toolkit to cluster, evaluate, and extract non-redundant associations of gene ontology-based functions. BMC Bioinformatics 2020; 21: 139.
[53] Kanehisa M, Furumichi M, Sato Y, Kawashima M and Ishiguro-Watanabe M. KEGG for taxonomy-based analysis of pathways and genomes. Nucleic Acids Res 2023; 51: D587-D592.
[54] Thul PJ and Lindskog C. The human protein atlas: a spatial map of the human proteome. Protein Sci 2018; 27: 233-244.
[55] Mizuno H, Kitada K, Nakai K and Sarai A. PrognoScan: a new database for meta-analysis of the prognostic value of genes. BMC Med Genomics 2009; 2: 18.